

# Ising model as Wilson-Majorana Fermions

Uli Wolff\*

Institut für Physik, Humboldt Universität

Newtonstr. 15

12489 Berlin, Germany

## Abstract

We show the equivalence of the 2D Ising model to standard free Euclidean lattice fermions of the Wilson Majorana type. The equality of the loop representations for the partition functions of both systems is established exactly for finite lattices with well-defined boundary conditions. The honeycomb lattice is particularly simple in this context and therefore discussed first and only then followed by the more familiar square lattice case.

## 1 Introduction

The two-dimensional Ising spin model can probably be called *the* prototype exactly solved model in statistical physics and lattice field theory. The break-through solution was achieved by Onsager [1] who has computed the partition function by the transfer matrix approach in 1944. Since then a large number of alternative – usually less complicated – strategies to derive the same result have been presented, like for instance [2]. Without any attempt toward completeness<sup>1</sup> we shall only mention below a few more selected references which are more or less close to our approach. Finally, we then hopefully will be able to sufficiently justify the present addition to this literature.

On a very naive level one may find the two-valuedness of the elementary spins reminiscent of fermionic states that can be empty and occupied. A much more concrete such link was established in the paper of Schultz, Mattis and Lieb [5]. The transfer matrix of the model is first expressed in terms of a tensor product

---

\*e-mail: uwolff@physik.hu-berlin.de

<sup>1</sup>A more extended recent collection of references is found in [3] for example. See also [4].

of Pauli algebras attached to the sites of a one dimensional row of the lattice. By performing a Jordan-Wigner transformation [6] the Pauli matrices are traded for anticommuting fermion operators. The transfer matrix in this form inherits the nearest neighbor bilinear structure of the original model and can hence be diagonalized by Fourier expansion on the lattice. Simpler analogous steps in the Hamiltonian limit of the transfer matrix (‘continuous time’) have later been discussed in [7] and [8].

An alternative to representing fermions by operators with canonical anticommutation relations is given by path integrals over anticommuting Grassmann ‘numbers’ [9]. Such a representation has been derived from the operator transfer matrix in [10]. Even earlier, Samuel [11] has used Grassmann integrals to directly ‘draw’ the high temperature series of the Ising model to all orders which constitutes an equivalent representation of the model. In either case the resulting integrals are Gaussian (free fermions), can be performed, and thus furnish an exact solution.

Samuel’s work is by far the closest to our work. The differences distinguishing the presentation at hand are however the following. We demonstrate the equivalence of the Ising model with free Euclidean Majorana fermions of the Wilson type [12] that is one of the standard choices in lattice field theory. The critical point corresponds to zero mass and the Euclidean relativistic invariance in the continuum/scaling limit is manifest in this standard framework. All phase factors in the matched expansions arise naturally from the fermion nature combined with half-angle spin rotation phases. The Fermi-Bose equivalence proven here will be an exact identity between arbitrary finite lattice partition functions with well-defined periodic or antiperiodic boundary conditions in each of the two lattice directions.

In section 2 the loop representation of the Ising model is defined and matched to the fermionic model for the honeycomb lattice. In section 3 the same program is implemented for the standard square lattice which is technically more complicated. Some conclusions and remarks on more than two dimensions are offered in section 4. In two appendices we report details on the evaluation of the spin weights and on the actual evaluation of the free fermion partition functions. In particular, the lattice fermion spectra are plotted.

## 2 Equivalence on the honeycomb lattice

### 2.1 Honeycomb geometry

The honeycomb lattice can be spanned by two triangular sublattices  $\mathcal{A}$  and  $\mathcal{B}$ , see figure 1. Each site  $x \in \mathcal{A}$  has three nearest neighbors  $x + \hat{e}_a \in \mathcal{B}$ ,  $a = 0, 1, 2$

where the three unit vectors<sup>2</sup> making 120 degree angles with each other fulfill

$$\hat{e}_a \cdot \hat{e}_b = \frac{1}{2}(3\delta_{ab} - 1). \quad (1)$$

The sites of  $\mathcal{A}$  are labeled by integers  $x_1, x_2$  in the form

$$\mathcal{A} \ni x = x_1 f_1 + x_2 f_2, \quad f_1 = \hat{e}_1 - \hat{e}_0, \quad f_2 = \hat{e}_2 - \hat{e}_0, \quad f_i \cdot f_j = \frac{3}{2}(\delta_{ij} + 1). \quad (2)$$

All sites in  $\mathcal{B}$  can now be generated as neighbors  $x + \hat{e}_0$  of a unique  $x \in \mathcal{A}$ .

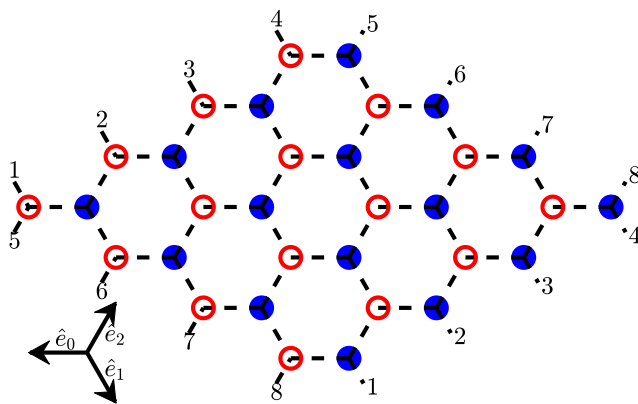


Figure 1: The honeycomb lattice with  $L_1 = L_2 = 4$ . Sites of  $\mathcal{A}(\mathcal{B})$  carry full blue (empty red) dots. Periodic boundary conditions are indicated by open links with equal indices.

A simple way to impose periodic boundary conditions<sup>3</sup> to obtain a finite system is to identify points  $x$  with  $x + L_1 f_1$  and  $x + L_2 f_2$  with integer  $L_i$ . We then have  $V = 2L_1 L_2$  independent sites in total, half in  $\mathcal{A}$  and half in  $\mathcal{B}$ .

We adopt the convention to take coordinates  $x_i \in [0, L_i)$  and label links by the pairs  $(x, a)$  with  $x \in \mathcal{A}$ ,  $a \in \{0, 1, 2\}$ . Which links close ‘around the boundary’?

<sup>2</sup>We use lattice units  $a = 1$  with respect to these nearest neighbor links.

<sup>3</sup>In [13] a more ‘rectangular’ periodicity is introduced that results in helical boundary conditions for the honeycomb fields. Clearly, also this case can be handled along the lines presented here.

The neighbors  $x + \hat{e}_a$  are in  $\mathcal{B}$  and in our coordinate system associated with (generated by)  $x + \hat{e}_a - \hat{e}_0$  back in  $\mathcal{A}$ , or in other words, with  $x, x + f_1, x + f_2$  which are folded back into the ranges  $[0, L_i)$  by standard modulo operations. A site  $y \in \mathcal{B}$  on the other hand is generated by  $y - \hat{e}_0 = z \in \mathcal{A}$  and its neighbors  $y - \hat{e}_a$  are  $z, z - f_1, z - f_2$ .

## 2.2 Ising model

We attach Ising spins  $s(x) \in \{+1, -1\}$  to all sites and write the partition function of the Ising model on the honeycomb lattice as

$$Z = \sum_s e^{\beta \sum_{a,x \in \mathcal{A}} s(x)s(x+\hat{e}_a)} = 2^V (\cosh \beta)^{3V/2} Z_r. \quad (3)$$

The reduced partition function  $Z_r$  is given by

$$Z_r = 2^{-V} \sum_s \prod_{a,x \in \mathcal{A}} (1 + ts(x)s(x + \hat{e}_a)), \quad t \equiv \tanh \beta. \quad (4)$$

We read off the loop graph representation of  $Z_r$  :

- we multiply out the big product and for each term draw lines on the links where the  $tss$  term is picked and leave empty links with factors one,
- after averaging each term over  $s$ , nonzero contributions arise only from graphs where each site is surrounded by an even number of lines,
- as each site has only 3 neighbors only zero or two lines are allowed at sites,
- therefore each nonzero contribution to  $Z_r$  can be seen as configuration of multiple non-intersecting closed loops,
- $Z_r$  is given by the sum over all different such loop gas configurations weighted with a factor  $t$  per line segment.

Symbolically we may write

$$Z_r = \sum_{\Lambda} t^{|\Lambda|}, \quad (5)$$

where the sum runs over the loop gas configurations on the lattice and  $|\Lambda|$  means the total number of links making up all the closed loops contained in  $\Lambda$ .

Up to here we have tacitly assumed periodic boundary conditions. For either or both of the directions  $f_1, f_2$  in which we close the torus, we may also take antiperiodic boundary conditions. We designate the 4 possible cases that arise by

bits  $\varepsilon_1, \varepsilon_2$  with  $\varepsilon_i = 0$  standing for periodic and  $\varepsilon_i = 1$  for antiperiodic. To detect if antiperiodicity leads to negative amplitudes we define winding numbers

$$q_i[\Lambda] = \text{number of occupied links}(x, i) |_{x_i=L_i-1} \pmod{2}. \quad (6)$$

Then, for generalized boundary conditions, the sign  $(-1)^{\varepsilon_1 q_1 + \varepsilon_2 q_2}$  has to be included in the sum in (5). The generalized Ising partition function with dynamical boundary conditions, in which we sum over the four cases with weights  $\rho(\varepsilon)$ , reads

$$Z_{I\rho} = \sum_{\Lambda} t^{|\Lambda|} \Phi_{\rho}[\Lambda] \quad \text{with} \quad \Phi_{\rho}[\Lambda] = \sum_{\varepsilon} \rho(\varepsilon) (-1)^{\varepsilon_1 q_1[\Lambda] + \varepsilon_2 q_2[\Lambda]}. \quad (7)$$

This enlarged ensemble, including a sum over boundary conditions, will be found to be a convenient starting point for the finite size equivalence to be derived.

### 2.3 Majorana Wilson fermion

We consider a two component Grassmann-valued field  $\xi_{\alpha}(x)$ ,  $\alpha = 1, 2$  living on the sites of the honeycomb lattice. It is endowed with the Gaussian Euclidean action

$$S = \frac{1}{2} \sum_x \bar{\xi}(x) \xi(x) - \kappa \sum_{a, x \in \mathcal{A}} \bar{\xi}(x) P(\hat{e}_a) \xi(x + \hat{e}_a) \quad (8)$$

written in the hopping parameter form. For a unit vector  $n$ ,  $P(n)$  is the Wilson projector

$$P(n) = \frac{1}{2} (1 - n_{\mu} \gamma_{\mu}). \quad (9)$$

The  $2 \times 2$  Dirac matrices generate the Clifford algebra

$$\{\gamma_{\mu}, \gamma_{\nu}\} = 2\delta_{\mu\nu}. \quad (10)$$

Note that  $\mu, \nu = 0, 1$  refer to a pair of orthogonal directions in the plane. Due to the Majorana nature of  $\xi$  the field  $\bar{\xi}(x)$  is not independent but given by

$$\bar{\xi} = \xi^{\top} \mathcal{C} \quad (11)$$

with the charge conjugation matrix  $\mathcal{C}$  defined by

$$\gamma_{\mu}^{\top} = -\mathcal{C} \gamma_{\mu} \mathcal{C}^{-1}. \quad (12)$$

In any representation one may prove antisymmetry,  $\mathcal{C} = -\mathcal{C}^{\top}$ , and our normalization will be  $\mathcal{C}_{12} = +1$ . We note that (8) contains a simple sum over all links. They are unoriented – as in the Ising model – because

$$\bar{\xi}(x) P(\hat{e}_a) \xi(x + \hat{e}_a) = \bar{\xi}(x + \hat{e}_a) P(-\hat{e}_a) \xi(x) \quad (13)$$

holds due to (12).

To study the so called naive continuum limit, we substitute  $\xi(x + \hat{e}_a) \simeq (1 + \hat{e}_a \cdot \partial)\xi(x)$ . Using the identities

$$\sum_a \hat{e}_a = 0, \quad \sum_a \hat{e}_{a,\mu} \hat{e}_{a,\nu} = \frac{3}{2} \delta_{\mu\nu} \quad (14)$$

we find

$$S \simeq \frac{3\kappa}{4} \sum_{x \in \mathcal{A}} \bar{\xi}(\gamma_\mu \partial_\mu + m)\xi \quad \text{with} \quad m = \frac{2}{\kappa}(2/3 - \kappa). \quad (15)$$

Hence, by rescaling  $\xi$  we have a canonical Majorana fermion of mass  $m$ . A small positive mass (in lattice units) appears as the hopping parameter  $\kappa$  approaches the critical value  $\kappa_c = 2/3$  from below. A discussion of the complete dispersion relation in momentum space and the exact partition function is given in appendix B.1

The fermion partition function is given by the Grassmann integral

$$Z_M = \int D\xi e^{-S} = \int D\xi \left\{ \prod_x \left( 1 - \frac{1}{2} \bar{\xi} \xi \right) \right\} \prod_{a,x \in \mathcal{A}} [1 + \kappa \bar{\xi}(x) P(\hat{e}_a) \xi(x + \hat{e}_a)]. \quad (16)$$

The integration over two Grassmann components per site factorizes  $D\xi = \prod_x d^2\xi$  and the local measure  $d^2\xi$  is taken such that

$$\int d^2\xi \xi_\alpha \bar{\xi}_\beta = \delta_{\alpha\beta} \quad \Rightarrow \quad \int d^2\xi (-) \frac{1}{2} \bar{\xi} \xi = 1. \quad (17)$$

Moreover, to arrive at the factorized form (16), the nilpotency of the Grassmann bilinears has been used, including the fact that  $P(\hat{e}_a)$  are one-dimensional projectors.

A moment of thought will reveal now, that upon executing the Grassmann integrations site by site and using (17) the same loop gas structure arises as from (4). For each loop  $\lambda$  the successive projectors  $P$  appear multiplied up and an over-all factor

$$w(\lambda) = -\text{tr}[P(n_1)P(n_2) \cdots P(n_N)]. \quad (18)$$

arises with  $n_1, n_2, \dots, n_N$  being the unit vectors  $\pm \hat{e}_a$  met on the links along the loop. The minus sign is the usual fermionic one: We order the commuting bilinears for the sequence of links in a loop schematically as  $\bar{\xi} P \xi \bar{\xi} P \xi \cdots \bar{\xi} P \xi$ . Successive inner pairs  $\xi \bar{\xi}$  are at the same site and integrate to  $\delta_{\alpha\beta}$ . The first  $\bar{\xi}$  and the last  $\xi$  similarly close the trace but come in the ‘wrong’ order, hence a factor  $-1$ . The geometric factor  $w$  is evaluated in detail in appendix A. For periodic boundary conditions in both directions, for example, we are led to

$$Z_M = \sum_\Lambda [\kappa \cos(\pi/6)]^{|\Lambda|} (2\delta_{q_1[\Lambda],0} \delta_{q_2[\Lambda],0} - 1). \quad (19)$$

Some further explanations are in order:

- Closed loops on the honeycomb lattice have as many 60 degree bends as they contain links. This results in the same powers of  $\kappa$  per link and  $\cos(\pi/6)$  per bend (half-angle between  $n_i$  and  $n_{i+1}$ , see (56)).
- For loops not winding around the torus, each Fermi sign is paired<sup>4</sup> with the spin minus from  $2\pi$  rotation (see appendix A). If  $\Lambda$  contains loops winding around one or both periodic directions (nonzero  $q_i$ ), the rotation is lacking and a minus sign is left.

For the superposition of boundary conditions with weight  $\eta(\varepsilon)$  the Majorana partition function becomes

$$Z_{M\eta} = \sum_{\Lambda} [\kappa \cos(\pi/6)]^{|\Lambda|} \Phi_{M\eta}[\Lambda] \quad (20)$$

with

$$\Phi_{M\eta}[\Lambda] = (2\delta_{q_1[\Lambda],0}\delta_{q_2[\Lambda],0} - 1) \sum_{\varepsilon} \eta(\varepsilon) (-1)^{\varepsilon_1 q_1[\Lambda] + \varepsilon_2 q_2[\Lambda]}. \quad (21)$$

We see that this loop gas coincides with (7) if the following matching conditions hold

$$\tanh \beta = t = \kappa \cos(\pi/6) = \frac{\sqrt{3}}{2} \kappa \quad (22)$$

and

$$\Phi_{\rho}[\Lambda] = \Phi_{M\eta}[\Lambda]. \quad (23)$$

The  $\Phi_{\times}$  depend on the graph  $\Lambda$  only through the winding numbers  $q_i[\Lambda]$  and their equality translates into a relation between  $\rho$  and  $\eta$  as follows. We may view  $\varepsilon_i$  and  $q_i$  as conjugate binary Fourier variables and invert

$$\rho(\varepsilon) = \frac{1}{4} \sum_q \Phi_{\rho}(q) (-1)^{\varepsilon_1 q_1 + \varepsilon_2 q_2}. \quad (24)$$

If we impose (23) this implies

$$\rho(\varepsilon) = \frac{1}{4} \sum_q (2\delta_{q_1,0}\delta_{q_2,0} - 1) \sum_{\varepsilon'} \eta(\varepsilon') (-1)^{\varepsilon'_1 q_1 + \varepsilon'_2 q_2} = 2\bar{\eta} - \eta(\varepsilon), \quad \bar{\eta} = \frac{1}{4} \sum_{\varepsilon} \eta(\varepsilon) \quad (25)$$

or the particularly symmetric form

$$\rho(\varepsilon) + \eta(\varepsilon) = 2\bar{\rho} = 2\bar{\eta}. \quad (26)$$

---

<sup>4</sup>It is this pairing that in our language makes two dimensional fermions special with an essentially positive loop representation.

By setting for example  $\rho(\varepsilon) = \delta_{\varepsilon, \varepsilon'}$  we obtain<sup>5</sup> for fixed boundary conditions (for either the Ising or the Majorana system)

$$Z_I(\beta, L_i, \varepsilon) + Z_M(\kappa, L_i, \varepsilon) = \frac{1}{2} \sum_{\varepsilon} Z_I(\beta, L_i, \varepsilon) = \frac{1}{2} \sum_{\varepsilon} Z_M(\kappa, L_i, \varepsilon) \quad (27)$$

with  $\beta, \kappa$  related by (22). Obviously, by taking derivatives, we may relate internal energy, susceptibility, etc. We have checked our formulas by exact summation on some small lattices. We remark that all  $Z_{\times}$  here are even in  $\beta$  or  $\kappa$ . This is shown by flipping the signs for all fields on one of the two sublattices.

Combining (22) with (15) the fermion mass (close to criticality) reads

$$m = 2 \frac{t_c - t}{t}, \quad t_c = \frac{1}{\sqrt{3}}, \quad \beta_c = \frac{1}{2} \ln(2 + \sqrt{3}). \quad (28)$$

Needless to say, the critical coupling of the Ising model on a honeycomb lattice has been well-known before, see references in [3]. We see that here the phase with  $\kappa > \kappa_c$  or  $m < 0$  of the free Wilson fermion corresponds to the magnetized  $Z(2)$  symmetry-broken Ising phase.

### 3 Equivalence on the square lattice

The Ising model is clearly most popular on the square lattice that we discuss now. It will turn out, however, that the loop representation and the Majorana form is a bit more complicated.

#### 3.1 Ising model

The formulas analogous to those in section 2.2 are rather obvious so that we here start immediately from the loop gas form which looks identical to (5) and (7) with just a re-definition of  $\Lambda$ . As before  $\Lambda$  is an arbitrary collection of line-carrying links such that an *even* number of lines touch any site of the torus. This allows for zero, two and, in contrast to the honeycomb lattice, also four links around a site. Because of the latter possibility, to be called crossings from here on, the configuration does in general not decompose into simple disjoint loops. By some abuse of language it is however customary to still talk about a loop gas configuration. The definition (6) can also be taken over unchanged if we substitute the orthogonal directions  $\mu = 0, 1$  for  $i = 1, 2$  and  $q_{\mu}[\Lambda]$  now are the corresponding modulo two winding numbers.

---

<sup>5</sup>Here the normalization of  $Z$  matters; we fix it by demanding  $Z_{\times} = 1$  for  $\beta = \kappa = 0$ .



### 3.2 Majorana Wilson fermion

The loop gas of a single species of Majorana Wilson fermions on the square lattice has been discussed in [14]. Attempting to ‘draw’ the Ising loop gas we notice two problems:

- crossings cannot occur with only two Grassmann components per site,
- 90 degree bends come with weight factors  $\cos(\pi/4) = 1/\sqrt{2}$  and their total power is not simply determined by the number of links as for the previous lattice. It can hence not be absorbed into the matching as before.

The decisive trick to solve both problems can be learned from [11]. We introduce two fields  $\xi_\mu(x)$  either of which has two spinor components. Now  $\xi_0$  has hopping terms in the zero direction only and  $\xi_1$  implements the perpendicular hops. Our Ansatz for a bilinear action is<sup>6</sup>

$$S = \sum_x s_0(\xi_\mu(x)) + \kappa \sum_{x,\mu} \bar{\xi}_\mu(x) P(\hat{\mu}) \xi_\mu(x + \hat{\mu}) \quad (29)$$

with unit vectors  $\hat{\mu}$  pointing in the positive  $\mu$  direction. To determine the on-site term  $s_0$  we postulate

$$\int d^4\xi e^{-s_0} \xi_{0,\alpha} \bar{\xi}_{0,\beta} = \int d^4\xi e^{-s_0} \xi_{1,\alpha} \bar{\xi}_{1,\beta} = \delta_{\alpha\beta} \quad (30)$$

to connect straight sections, and

$$\int d^4\xi e^{-s_0} \xi_{0,\alpha} \bar{\xi}_{1,\beta} \equiv \int d^4\xi e^{-s_0} \xi_{1,\alpha} \bar{\xi}_{0,\beta} = \sqrt{2} \delta_{\alpha\beta} \quad (31)$$

to cancel the corner weights. A short calculation shows that this is uniquely achieved by the quadratic form

$$s_0 = \frac{1}{2}(\bar{\xi}_0 \xi_0 + \bar{\xi}_1 \xi_1) - \sqrt{2} \bar{\xi}_0 \xi_1. \quad (32)$$

A novelty arises for the empty sites. They now contribute minus signs to the loop amplitude because we find

$$\int d^4\xi e^{-s_0} = -1. \quad (33)$$

The integral with all four Grassmann components is now determined and reads

$$\int d^4\xi e^{-s_0} \xi_{0\alpha} \bar{\xi}_{0\beta} \xi_{1\gamma} \bar{\xi}_{1\delta} = \delta_{\alpha\beta} \delta_{\gamma\delta}. \quad (34)$$

We find that at crossings the ‘vertical’ pair gets connected by spin contraction as well as the ‘horizontal’ one, see figure 2. Hence in this case we now do find separate closed loops, with intersections (including self-intersections of the same loop) allowed.

---

<sup>6</sup>The unusual sign of  $\kappa$  will turn out to be convenient later.

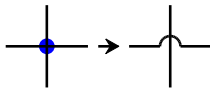


Figure 2: Visualization of the spin contractions at crossings.

The partition function at fixed boundary conditions  $\varepsilon$  now reads

$$Z_M(\kappa, L_\mu, \varepsilon) = \int D\xi e^{-S} = \sum_{\Lambda} \kappa^{|\Lambda|} (-1)^{\varepsilon_0 q_0[\Lambda] + \varepsilon_1 q_1[\Lambda]} (2\delta_{q_0[\Lambda], 0} \delta_{q_1[\Lambda], 0} - 1). \quad (35)$$

The sign (33) has been absorbed here into  $D\xi = \prod_x (-d^4\xi(x))$  to adhere to the normalization  $Z_M(0, L_\mu, \varepsilon) = 1$ . This however implies now extra signs at all non-empty sites, i.e. connections as well as the crossings (34). In addition the hopping terms come with factors  $(-\kappa)$ . In this way for a graph *without* crossings, which visits the same number  $|\Lambda|$  of links and sites, these signs cancel. For each crossing there first seems an extra minus left over. If a crossing is a self-intersection, this extra sign cancels however with an extra  $2\pi$  rotation collected along the corresponding line, which, if it does not run around the torus, then contributes a total plus sign. If the crossing is between separate loops, there always is an even number of them.

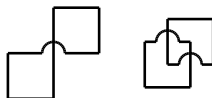


Figure 3: Examples of self-intersection and intersections of separate loops.

We try to visualize this in figure 3. In this way the number of crossings  $n_+[\Lambda]$  does not appear in the final weight, which is essential to be able to match the Ising loop gas. The condition for this is given by

$$\tanh \beta = \kappa \quad (36)$$

for the square lattice. The relation (27) between partition functions holds unchanged. The factor in the last bracket in (35) has the same reason as discussed for the honeycomb lattice. We finally re-emphasize that the loop configurations  $\Lambda$  in (35) are the same as those described in section (3.1). The exact evaluation of the partition function (35) by performing the Gaussian Grassmann integral is discussed in appendix B.2.

If both  $L_0$  and  $L_1$  are even, also the square lattice is bi-partite and partition functions are even in  $\beta$  or  $\kappa$  respectively. If we also allow for odd lattice lengths the generalized relation

$$Z_M(-\kappa, L_\mu, \varepsilon) = Z_M(\kappa, L_\mu, \varepsilon^{(L)}) \quad (37)$$

can be proven with

$$\varepsilon_\mu^{(L)} = \varepsilon_\mu + L_\mu \pmod{2}, \quad (38)$$

i. e. a swap between periodic and antiperiodic for odd  $L_\mu$  directions.

For an easier interpretation of the continuum limit of the action (29) we diagonalize  $s_0$  by changing to new fields  $\eta$  and  $\chi$

$$\xi_0 = \frac{i}{\sqrt{\kappa}}(\eta + \chi), \quad \xi_1 = \frac{i}{\sqrt{\kappa}}(\eta - \chi). \quad (39)$$

Introducing the forward, backward and symmetric difference operators  $\partial_\mu$ ,  $\partial_\mu^*$  and  $\tilde{\partial}_\mu$ , the action reads

$$\begin{aligned} S = & \frac{1}{2} \sum_x \bar{\eta} \left( m_\eta + \gamma_\mu \tilde{\partial}_\mu - \frac{1}{2} \partial_\mu \partial_\mu^* \right) \eta + \frac{1}{2} \sum_x \bar{\chi} \left( m_\chi + \gamma_\mu \tilde{\partial}_\mu - \frac{1}{2} \partial_\mu \partial_\mu^* \right) \chi \\ & + \sum_x \bar{\eta} \left( \gamma_0 \tilde{\partial}_0 - \gamma_1 \tilde{\partial}_1 - \frac{1}{2} \partial_0 \partial_0^* + \frac{1}{2} \partial_1 \partial_1^* \right) \chi \end{aligned} \quad (40)$$

with

$$m_\eta = \frac{2}{\kappa} \left[ \sqrt{2} - 1 - \kappa \right], \quad m_\chi = -\frac{2}{\kappa} \left[ \sqrt{2} + 1 + \kappa \right]. \quad (41)$$

The standard Ising critical point appears at

$$m_\eta = 0 \quad \Leftrightarrow \quad \kappa = \kappa_c = \tanh \beta_c = \sqrt{2} - 1 \quad \Rightarrow \quad \beta_c = \frac{1}{2} \ln \left( \sqrt{2} + 1 \right) \quad (42)$$

While the field  $\eta$  is critical here and acquires long range correlations we have a large negative mass in lattice units  $m_\chi = -4(2 + \sqrt{2})$ . Hence the coupling to this field only contributes small lattice corrections to the Euclidean symmetric Majorana ‘particles’ described by  $\eta$ . As before small positive  $m_\eta$  ( $\kappa < \kappa_c$ ) corresponds to the symmetric Ising phase with the ferromagnetic one being on the other side at negative  $m_\eta$  ( $\kappa > \kappa_c$ ).

The two fields swap their roles at

$$m_\chi = 0 \quad \Leftrightarrow \quad \kappa = \kappa'_c = \tanh \beta'_c = -\sqrt{2} - 1 \quad \Rightarrow \quad \beta'_c = -\beta_c \pm i\frac{\pi}{2} \quad (43)$$

with  $m_\eta = -4(2 - \sqrt{2})$  in this case.

### 3.3 Relation with reference [11]

In [11] Samuel has employed Grassmann variables to reproduce the low temperature expansion of the Ising model (Bloch walls) in powers of<sup>7</sup>  $z = \exp(-2\beta)$ . As the 2-dimensional model on the square lattice is self-dual, this coincides with the high temperature  $\tanh \beta$  expansion (finite size effects are disregarded in [11]).

In a first step we adapt Samuels notation for the Grassman fields by replacing

$$(\eta^{h^x}, -\eta^{h^o}, \eta^{v^x}, -\eta^{v^o}) \rightarrow (\eta_{01}, \eta_{02}, \eta_{11}, \eta_{12}), \quad (44)$$

and temporarily assume gamma matrices  $\gamma_0 = \tau_3$ ,  $\gamma_1 = \tau_1$  in terms of Pauli matrices. The action (3.4) in [11] for the Ising case now translates to

$$A = -z \sum_{x\mu} \bar{\eta}_\mu(x) P(\hat{0}) \eta_\mu(x + \hat{\mu}) - \frac{1}{2} \sum_{x\mu} \bar{\eta}_\mu \eta_\mu + \sum_x \bar{\eta}_0 (1 + \mathcal{C}^{-1}) \eta_1, \quad (45)$$

where spin summations are implicit again. To bring the hopping terms into the same form as in (29), we perform a spinor rotation  $\eta_1 \rightarrow R\eta_1$  with  $R = \exp(i\pi\tau_2/4)$  which yields  $R^\dagger \gamma_0 R = \gamma_1$ . In terms of these fields the total action now reads

$$A = -z \sum_{x\mu} \bar{\eta}_\mu(x) P(\hat{\mu}) \eta_\mu(x + \hat{\mu}) - \frac{1}{2} \sum_x \bar{\eta} \eta + \sum_x \bar{\eta}_0 (1 + \mathcal{C}^{-1}) R \eta_1. \quad (46)$$

Using now  $\mathcal{C} = i\tau_2$  and  $R = (1 + i\tau_2)/\sqrt{2}$  we find complete agreement with the manifestly (cubic) rotation invariant form (29).

## 4 Conclusions and outlook

We have given an exact mapping between the Ising model and free Majorana Wilson fermions for finite honeycomb and square lattices. The critical point occurs at vanishing mass  $m$  or, equivalently, the critical hopping parameter  $\kappa_c$ . Although trivial, we mention that the equivalence with free fermions immediately explains the value  $\nu = 1$  for the correlation length exponent as this scale is given by the

---

<sup>7</sup>We take  $z_h = z_v = z$  for simplicity.

inverse mass. The magnetized phase with broken  $Z(2)$  symmetry corresponds to  $\kappa > \kappa_c$  or negative mass.

The question of extensions to three dimensions comes to mind. There is a lattice with coordination number three, the so-called hydrogen-peroxide lattice [15]. The loop expansion of the three dimensional Majorana Wilson fermion worked out in [14] for the cubic lattice can be adapted to this case by just eliminating a fraction of the links. Then the graphs ‘drawn’ by the free fermions would indeed coincide with those of the  $\tanh \beta$  expansion of the Ising model, namely a gas of non-intersecting closed loops. However, as explicitly worked out in [14], any such fermion graph containing non-planar loops comes with spin phase factors in the group  $Z(8)$  – related to cubic lattice rotations – which oscillate in an essential way. Therefore, the graph weights *cannot* be matched in this case.

## A Spin factor

The calculation in this appendix closely follows the arguments given in appendix B of [14], but is generalized here beyond the square lattice.

We consider a single closed loop  $\lambda$  of length  $N$  on a 2 dimensional lattice to be associated with a sequence of lattice unit vectors  $n_i, i = 1, 2, \dots, N$  which connect nearest neighbors and add to zero

$$\sum_{i=1}^N n_i = 0. \quad (47)$$

For a given starting point  $x_0$  on the lattice, all points recursively given by  $x_i = x_{i-1} + n_i$  are nearest neighbor lattice sites until the loop closes at  $x_N = x_0$ . The spin factor associated with such a loop  $\lambda$  is given by the traced product of Wilson projectors (18) where the additional Fermi minus is included. Note that  $w$  is invariant under cyclic changes of the  $n_i$  and under inversions due to (12). Hence neither the starting point along the loop nor the chosen orientation matters for  $w$ , which thus is a function of the unoriented loop.

For the evaluation of  $w$  we note each pair of  $n_i, n_j$  can be rotated into each other. Using the spinor representation this allows us to write

$$P(n_{i+1}) = R_i^{-1} P(n_i) R_i \quad (48)$$

with

$$R_i = \exp\left(\frac{\alpha_i}{2} \gamma_0 \gamma_1\right) \quad \text{with} \quad \cos(\alpha_i) = n_i \cdot n_{i+1}. \quad (49)$$

This is used, starting from the rightmost factors in the product,

$$P(n_{N-1})P(n_N) = P(n_{N-1})R_{N-1}^{-1}P(n_{N-1})R_{N-1} = \cos(\alpha_{N-1}/2)P(n_{N-1})R_{N-1} \quad (50)$$

where we have used  $P \exp(\alpha \gamma_0 \gamma_1) P = \cos(\alpha) P$ . Upon iteration we arrive at

$$w(\lambda) = - \left\{ \prod_{i=1}^{N-1} \cos(\alpha_i/2) \right\} \text{tr}[P(n_1) R_1 R_2 \cdots R_{N-1}]. \quad (51)$$

If we define the additional rotation  $R_N$  to achieve

$$P(n_1) = R_N^{-1} P(n_N) R_N, \quad (52)$$

then the total rotation

$$R_\lambda = R_1 R_2 \cdots R_{N-1} R_N \quad (53)$$

has the direction  $n_N$  as a fixed point

$$P(n_N) = R_\lambda^{-1} P(n_N) R_\lambda \quad (54)$$

which implies

$$R_\lambda = \exp \left( \gamma_0 \gamma_1 \frac{1}{2} \sum_{i=1}^N \alpha_i \right) = \pm 1 \quad (55)$$

and

$$w(\lambda) = -R_\lambda \prod_{i=1}^N \cos(\alpha_i/2). \quad (56)$$

For simple non-selfintersecting contractable closed loops in the plane the angles  $\alpha_i$  add up to  $2\pi$  and thus  $R_\lambda = -1$  holds. This clearly is the minus sign under a  $2\pi$  rotation that a spinor receives as it is transported once around the closed loop. Note that this does not occur for loops closing around the torus in one or both directions. Bends along the loops are suppressed by weight factors  $\cos(\pi/6) = \sqrt{3}/2$  (honeycomb) and  $\cos(\pi/4) = 1/\sqrt{2}$  (square).

## B Exact dispersion of Wilson fermions

### B.1 Honeycomb lattice

We switch to sublattice Majorana fields

$$\chi(x) = (\chi_A(x), \chi_B(x)) \equiv (\xi(x), \xi(x + \hat{e}_0)) \quad (57)$$

with the 4-component field  $\chi$  attached to sublattice  $\mathcal{A}$ . We write down a Fourier representation

$$\chi(x) = \frac{1}{L_1 L_2} \sum_p \tilde{\chi}(p) e^{i(p_1 x_1 + p_2 x_2)}. \quad (58)$$

Some straightforward algebra yields the action (8) in terms of  $\tilde{\chi}$

$$S = \frac{1}{2L_1L_2} \sum_p \{ \tilde{\chi}(-p)\tilde{\chi}(p) - \kappa[\tilde{\chi}_A(-p)M_+\tilde{\chi}_B(p) + \tilde{\chi}_B(-p)M_-\tilde{\chi}_A(p)] \} \quad (59)$$

with

$$M_{\pm}(p) = \sum_{j=0}^2 P(\pm\hat{e}_j)e^{\pm ip_j} \quad (p_0 \equiv 0). \quad (60)$$

The momenta to be summed over depend on the lattice size  $L_i$  and (anti)periodicity  $\varepsilon_i$ . A possible choice would be  $p_i = (2\pi/L_i)(\varepsilon_i/2 + n_i)$ ,  $n_i = 0, \dots, L_i - 1$ . The special values  $p_i = 0$  are allowed for  $\varepsilon_i = 0$  and  $p_i = \pi$  occurs if  $L_i + \varepsilon_i$  is even. If all components are of this type,  $p$  and  $-p$  are identical<sup>8</sup> and so are  $\tilde{\chi}(p)$  and  $\tilde{\chi}(-p)$ . The Grassmann integral for such momenta then leads to a Pfaffian of the quadratic form defined by (59). The remaining momenta come in pairs associated with independent Grassmann fields and contribute determinant factors to the partition function, one per pair. We divide up the set of all momenta as follows,

$$\mathcal{B}(L_i, \varepsilon_i) = \mathcal{B}_0(L_i, \varepsilon_i) \cup \mathcal{B}_+(L_i, \varepsilon_i) \cup \mathcal{B}_-(L_i, \varepsilon_i), \quad (61)$$

where  $\mathcal{B}_0$  contains momenta made of components 0 or  $\pi$  only, while  $\mathcal{B}_+$  contains *one member* of each of the remaining pairs  $\pm p$  with the partner momenta in  $\mathcal{B}_-$ . This implies for the cardinalities  $|\mathcal{B}_0| + 2|\mathcal{B}_+| = L_1L_2$  to hold.

In any case we may perform half of the Gaussian integrations - say over  $\tilde{\chi}_B$  - to obtain the reduced action

$$S_A = \frac{1}{2L_1L_2} \sum_p \{ \tilde{\chi}_A(-p) \{ 1 - \kappa^2 M_+ M_- \} \tilde{\chi}_A(p) \} \quad (62)$$

which leads to  $2 \times 2$  determinants and Pfaffians. We expand

$$M_+ M_- = a + ib_{\mu} \gamma_{\mu} + ic \gamma_0 \gamma_1 \quad (63)$$

and find in a short calculation

$$a = \frac{3}{4} \{ \cos(p_1) + \cos(p_2) + \cos(p_1 - p_2) \}, \quad (64)$$

$$b = \frac{1}{2} \{ \sin(p_1) f_1 + \sin(p_2) f_2 + \sin(p_1 - p_2) (f_1 - f_2) \}, \quad (65)$$

$$c = \frac{\sqrt{3}}{4} \{ -\sin(p_1) + \sin(p_2) + \sin(p_1 - p_2) \}. \quad (66)$$

---

<sup>8</sup> $p_i$  differing by multiples of  $2\pi$  are identified, of course.

This implies for the determinants

$$D(p) = (1 - \kappa^2 a)^2 + \kappa^4 (b_\mu b_\mu - c^2). \quad (67)$$

For momenta in  $\mathcal{B}_0$  the contributions  $b_\mu$  and  $c$  vanish and the Pfaffian is given by

$$P(p) = 1 - \kappa^2 a \quad (p_\mu \in \{0, \pi\}). \quad (68)$$

Note that  $P^2 = D$  holds here, but the root of  $D$  has to be taken such, that  $P$  is a polynomial in  $\kappa$ . In total we arrive at

$$Z_M(\kappa, L_i, \varepsilon_i) = \left\{ \prod_{p \in \mathcal{B}_0(L_i, \varepsilon_i)} P(p) \right\} \prod_{p \in \mathcal{B}_+(L_i, \varepsilon_i)} D(p). \quad (69)$$

The four eigenvalues  $\lambda = 1 + \kappa\rho$  (for each  $p$ ) of the quadratic form (59), which control the fermion two-point function, are given by

$$\rho = \pm \sqrt{a \pm \sqrt{c^2 - b_\mu b_\mu}} \quad (4 \text{ sign combinations}). \quad (70)$$

The spectrum of complex  $\rho$  values is shown in figure 4. The spectral radius  $3/2$  corresponds to the critical values  $\kappa_c = 2/3$ . The spectrum is invariant under  $\rho \rightarrow \rho^*$  as one can show  $M_\pm^* = \mathcal{C}M_\mp \mathcal{C}^{-1}$ , and under  $\rho \rightarrow -\rho$  that is related to the  $\kappa \rightarrow -\kappa$  symmetry. The arc of eigenvalues tangent to the dashed line in figure 4 approximates the imaginary spectrum of the continuum Euclidean Dirac operator  $\gamma_\mu \partial_\mu$ .

Upon expanding for small  $p_1, p_2$  one finds that  $a$  and  $b_\mu b_\mu$  depend on the combination  $p_1^2 + p_2^2 - p_1 p_2$  while  $c$  only contributes to higher orders. To arrive at the Fourier form (58) we actually expand  $p = p_1 \tilde{f}_1 + p_2 \tilde{f}_2$  in the basis dual to (2) which is defined by  $f_i \cdot \tilde{f}_j = \delta_{ij}$ . Then by elementary steps we find

$$p^2 = \frac{4}{9}(p_1^2 + p_2^2 - p_1 p_2). \quad (71)$$

Hence this combination is Euclidean invariant in our basis and so is the free energy and the dispersion in the continuum limit.

## B.2 Square lattice

The action in momentum space can be written as

$$S = \frac{1}{2L_0 L_1} \sum_p \left\{ \sum_\mu \tilde{\xi}_\mu(-p) [1 + \kappa e^{-ip_\mu \gamma_\mu}] \tilde{\xi}_\mu(p) - \sqrt{2} [\tilde{\xi}_0(-p) \tilde{\xi}_1(p) + \tilde{\xi}_1(-p) \tilde{\xi}_0(p)] \right\} \quad (72)$$



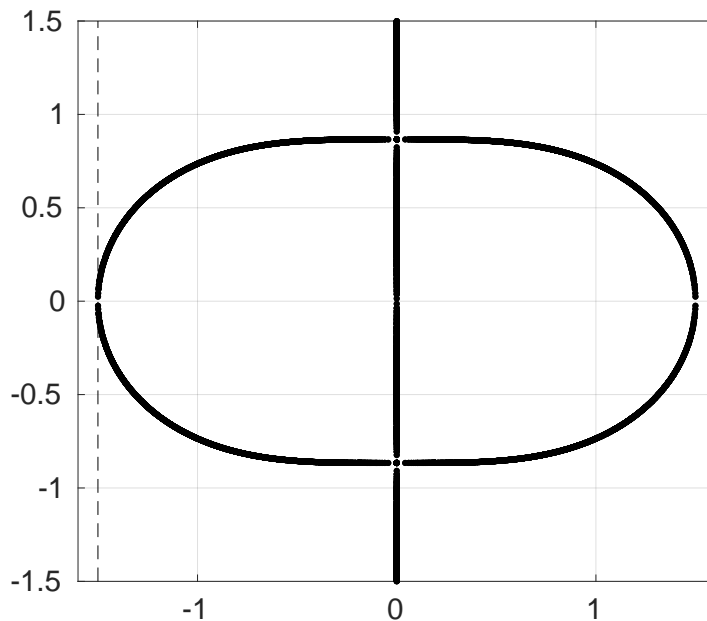


Figure 4: Fermion spectrum  $\rho$  for  $L_1 = L_2 = 64$  and antiperiodic boundary conditions.

By similar manipulations as in the previous subsection we may work out the characteristic polynomial whose zeros are the eigenvalues of the quadratic form defined by (72),

$$C(\lambda) = \sum_{i=0}^4 c_i (1 - \lambda)^i, \quad (73)$$

with

$$\begin{aligned} c_4 &= 1 \\ c_3 &= 2\kappa[\cos(p_0) + \cos(p_1)] \\ c_2 &= 2\kappa^2[1 + 2\cos(p_0)\cos(p_1)] - 4 \\ c_1 &= 2\kappa(\kappa^2 - 2)[\cos(p_0) + \cos(p_1)] \\ c_0 &= \kappa^4 + 4[1 - \kappa^2\cos(p_0)\cos(p_1)] \end{aligned}$$

While closed expressions for the eigenvalues can be given now, we found them not very illuminating and content ourselves with figure 5 for  $\kappa = \pm\sqrt{2} - 1$ . The dashed vertical lines are tangent to approximate continuum spectra of  $\gamma_\mu\partial_\mu$ . One

shows invariance of the spectrum under  $\lambda \rightarrow \lambda^*$  due to the property  $(e^{-ip_\mu\gamma_\mu})^* = \mathcal{C}e^{-ip_\mu\gamma_\mu}\mathcal{C}^{-1}$ . The symmetry  $\lambda \rightarrow 2 - \lambda$  holds for even  $L_\mu$  or requires a simultaneous change in the boundary conditions as in (38).

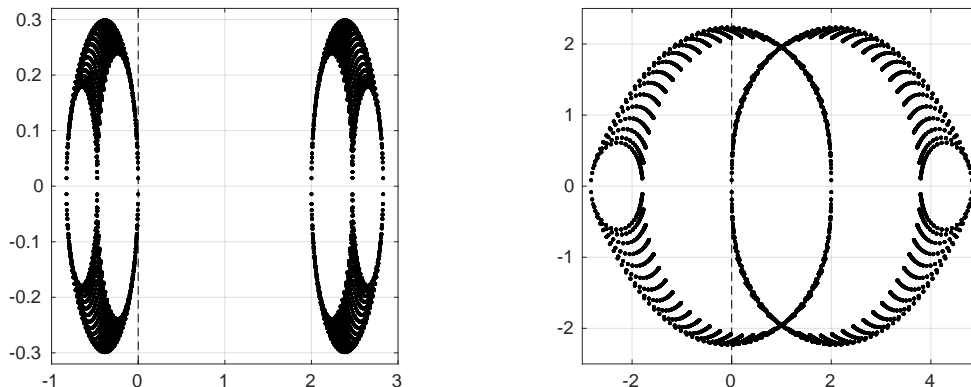


Figure 5: Eigenvalues  $\lambda$  for  $L_\mu = 64$  and antiperiodic boundary conditions for  $\kappa = \sqrt{2} - 1$  (left plot) and  $\kappa = -\sqrt{2} - 1$  (right plot).

To compute  $Z_M$  the momenta are divided as in the previous subsection and the Grassmann integrations again lead to Pfaffians and determinants. The result is

$$Z_M(\kappa, L_\mu, \varepsilon_\mu) = \left\{ \prod_{p \in \mathcal{B}_0(L_\mu, \varepsilon_\mu)} P(p) \right\} \prod_{p \in \mathcal{B}_+(L_\mu, \varepsilon_\mu)} D(p) \quad (74)$$

with

$$D(p) = C(0) = (1 + \kappa^2)^2 + 2\kappa(\kappa^2 - 1)[\cos(p_0) + \cos(p_1)] \quad (75)$$

and for  $p \in \mathcal{B}_0$  we find the Pfaffians

$$P(p) = \begin{cases} 2 - (1 + \kappa)^2 & \text{for } p = (0, 0) \\ 1 + \kappa^2 & \text{for } p = (\pi, 0), (0, \pi) \\ 2 - (1 - \kappa)^2 & \text{for } p = (\pi, \pi) \end{cases} \quad (76)$$

For small  $p_\mu$  we obviously find the dependence on the relativistic invariant  $p_0^2 + p_1^2$  at leading order in all terms.

## References

- [1] L. Onsager, *Crystal Statistics. I. A Two-Dimensional Model with an Order-Disorder Transition*, *Phys. Rev.* **65** (1944).

- [2] B. Kaufman, *Crystal Statistics. 2. Partition Function Evaluated by Spinor Analysis*, *Phys. Rev.* **76** (1949) 1232.
- [3] J. Strecka and M. Jascur, *A brief Account of the Ising and Ising-like Models: Mean Field, Effective-Field and exact Results*, *Acta Physica Slovaca* **65** (2015) [arXiv:1511.0303].
- [4] B. McCoy and T. Wu, *The two-dimensional Ising model*. Harvard University Press, 1973.
- [5] T. D. Schultz, D. C. Mattis, and E. H. Lieb, *Two-dimensional Ising model as a soluble problem of many fermions*, *Rev. Mod. Phys.* **36** (1964) 856.
- [6] P. Jordan and E. P. Wigner, *Über das Paulische Äquivalenzverbot*, *Zeit. Phys.* **47** (1928) 631.
- [7] P. Pfeuty, *The one-dimensional Ising model with a transverse field*, *Annals of Physics* **57** (1970) 79.
- [8] J. B. Kogut, *An Introduction to Lattice Gauge Theory and Spin Systems*, *Rev. Mod. Phys.* **51** (1979) 659.
- [9] F. A. Berezin, *The method of Second Quantization*. Academic Press, New York, 1966.
- [10] C. Itzykson, *Ising Fermions. 1. Two-Dimensions*, *Nucl. Phys.* **B210** (1982) 448.
- [11] S. Samuel, *The use of anticommuting integrals in statistical mechanics. 1*, *J. Math. Phys.* **21** (1980) 2806.
- [12] K. G. Wilson, *Quarks and Strings on a Lattice*, in *New Phenomena in Subnuclear Physics: Proceedings, International School of Subnuclear Physics, Erice, Sicily, Jul 11-Aug 1 1975. Part A*, p. 99, 1975.
- [13] D. Smith and L. von Smekal, *Monte-Carlo simulation of the tight-binding model of graphene with partially screened Coulomb interactions*, *Phys.Rev.B* **89** (2014), no. 19 195429, [arXiv:1403.3620].
- [14] U. Wolff, *Simulating the All-Order Hopping Expansion II: Wilson Fermions*, *Nucl. Phys.* **B814** (2009) 549, [arXiv:0812.0677].
- [15] Q.-Q. Liu, Y. Deng, T. M. Garoni, and H. W. Blote, *The  $O(n)$  loop model on a three-dimensional lattice*, *Nucl.Phys.* **B859** (2012) 107–128, [arXiv:1112.5647].